10.47952/gro-publ-199

Modeling CT images in the presence of beam hardening

Tamás Dózsa, Sándor Fridli, Péter Kovács

***Abstract*—We propose a parameterized mathematical model to approximate CT images in the presence of beam hardening. This physical phenomenon causes so-called cupping and streaking artifacts to appear on the reconstructed image. We pose the problem of optimizing the model parameters as a separable nonlinear least squares approximation task. The optimized model parameters have exact physical meaning. More precisely, the model parameters can be used to describe the attenuation properties of different materials with respect to monochromatic components of polychromatic X-ray beams. In addition, the proposed model can be used to correct the reconstructed image in a physically informative way. We find that the proposed method provides reliable estimates of the examined object's attenuation properties up to 4 dominant beam components. We verify the proposed method's effectiveness through numerical simulations.**

***Index Terms*—Computer Tomography, Variable Projection, Adaptive signal models, Separable Nonlinear Least Squares**

I. Introduction

Computer tomography (CT) has been an indispensable tool for examining the internal structure of objects since its introduction in 1972 [1]. The use of CT images is prevalent across a wide array of applications such as medical imaging [1], [2], [3] and non-intrusive structural analysis in industrial settings [4], [5]. CT machines emit X-ray beams that pass through the object of interest. As the beams traverse through the object, they are attenuated. Since different materials attenuate beams to a different extent, beam intensities are measured before and after they pass through the object. This process is repeated many times, with the emitter-detector pairs rotated around the object yielding a 3-D reconstruction of the internal structure [1], [2], [3] (see fig 1).

In practice, many problems can occur during the scanning process which cause artifacts to appear in the reconstructed image. These can be divided into several categories [1]. In this work, we consider the modeling and correction of artifacts which appear because of a physical phenomenon known as beam hardening [1], [6], [7], [8], [9], [10], [11]. This phenomenon occurs, because the attenuation properties of a material also depend on the energy level of the photons which make up the X-ray beams. Lower energy photons are more easily attenuated, thus the presence of this phenomenon causes so-called "cupping" and "streaking" in the reconstructed images (see Fig. 2).

Tamás Dózsa, Sándor Fridli, Péter Kovács are with ELTE Eötvös Loránd University, Faculty of Informatics, Department of Numerical Analysis, Budapest, Hungary, email: dotuaai@inf.elte.hu, fridli@inf.elte.hu, kovika@inf.elte.hu

Tamás Dózsa is also with the HUN-REN Institute for Computer Science and Control

The correction of beam hardening artifacts is an intensively studied problem [6], [7], [8], [9], [10], [11], [12]. The most popular existing methods can be divided into two main categories. Physical methods involve placing a highly attenuating material in front of the emitters to filter high frequency beam components and artificially "harden" the beam [12]. Drawbacks of this approach include the need to physically modify the CT machine as well as a reduction in the scan's quality especially for low dose methods.

In contrast, software based correction methods usually consider artifact removal as a post processing step of CT imaging [6], [7], [8], [9], [10], [11]. These approaches can be divided into three large subcategories: linearization [6], [9], dual energy [7], [10] and iterative methods [8], [11], [13]. Each of these approaches have their advantages, however iterative methods can be applied in more general settings (see e.g. [13]).

In [13], we proposed an iterative method for the correction of artifacts caused by beam hardening. The main novelty of our approach was that for homogeneous materials, the method could be used to not only correct, but also to estimate the true attenuation properties of the examined object at each beam energy level. This property is a significant advantage over previous methods, which could only be used to remove the beam hardening artifacts. Since these methods (see e.g. [8] and also [13]) did not provide precise estimates of the attenuation parameters, the corrected images could only be used to conduct a relative comparison of the attenuation properties of the materials present in the object. For objects containing multiple materials, in [13] we proposed a simplification of an existing method [8], however we could not claim the precise estimation of the attenuation properties of each material at each energy level.

In this work, we extend our results in [13] to objects made up of multiple materials. The proposed method can be used to estimate the attenuation of the entire object at each energy level. Thus, the corrected images also contain relevant information about the attenuation properties of the examined object. This behavior is preferable in both medical and industrial settings.

The rest of this paper is organized as follows. In section II, we review some mathematical concepts needed to optimize the parameters of the proposed method. Section III reviews the fundamental equations used to model the beam hardening. In section IV, we propose a parameterized model and discuss how it can be used to correct beam hardening artifacts. Section V contains the results of our numerical experiments and their discussion. Finally, we draw our conclusions and discuss future research directions in section VI.

II. Variable projection operators

In section IV, we derive our proposed model from a discrete variation of the Beer-Lambert law (see e.g. [1]). That is, we propose a parameterized model, where a good approximation of the cupping artifact ridden CT image can be obtained through the appropriate choice of the model parameters. An important component of the proposed algorithm is to formalize this nonlinear optimization problem as a so-called separable nonlinear least squares (SNLLS) task [14], [15]. In this section, we briefly introduce SNLLS problems and the related variable projection operators [14], [15].

Suppose $\mathcal{H}$ is a Hilbert space, and the elements $\varphi_0, \dots, \varphi_{m-1} \in \mathcal{H}$ $(m \in \mathbb{N})$ form a linearly independent system that spans an m-dimensional subspace $\mathcal{U} \subset \mathcal{H}$. Let $f \in \mathcal{H}$ be arbitrary. It is well known (see e.g. [16]), that there exists a unique element $\hat{f} \in \mathcal{U}$, that falls closest to f, that is $\|f - \hat{f}\|$ is minimal, where $\|\cdot\|$ denotes the norm induced by the inner product in $\mathcal{H}$. Since $\langle f - \hat{f}, g\rangle = 0$ $(g \in \mathcal{U})$ also holds, $\hat{f}$ is referred to as *the orthogonal projection* of f onto $\mathcal{U}$.

Suppose now, that the elements of the basis $\varphi_0^{\boldsymbol{\eta}}, \varphi_1^{\boldsymbol{\eta}}, \dots, \varphi_{m-1}^{\boldsymbol{\eta}} \in \mathcal{H}$ also depend on the real parameter vector $\boldsymbol{\eta} \in \mathbb{R}^q$, $q \in \mathbb{N}$. This means that the subspace $\mathcal{U}(\boldsymbol{\eta}) = \text{span}\{\varphi_0^{\boldsymbol{\eta}}, \varphi_1^{\boldsymbol{\eta}}, \dots, \varphi_{m-1}^{\boldsymbol{\eta}}\} \subset \mathcal{H}$ and in turn, the best approximation $\hat{f}(\boldsymbol{\eta})$ also depend on $\boldsymbol{\eta}$. Clearly, $\hat{f}(\boldsymbol{\eta})$ exists for any fixed $\boldsymbol{\eta}$. We call the operator $P^{\boldsymbol{\eta}} : \mathcal{H} \to \mathcal{U}(\boldsymbol{\eta})$ defined as

$$P^{\boldsymbol{\eta}} f := \hat{f}(\boldsymbol{\eta})$$

a variable projection operator [14], [15].

In real-world applications [15], specific Hilbert spaces and parameterized bases are considered. For the CT image modeling problem, we are going to use the Hilbert space $L_2(\mathbb{R})$. More specifically, we are going to consider the CT measurements as discrete samplings of $L_2(\mathbb{R})$ functions. That is, we will assume $\mathcal{H} := \mathbb{R}^N$. Suppose the columns of the matrix $\Phi(\boldsymbol{\eta}) \in \mathbb{R}^{N \times m}$ contains discrete samplings of the basis functions $\varphi_0^{\boldsymbol{\eta}}, \dots \varphi_{m-1}^{\boldsymbol{\eta}} \in L_2(\mathbb{R})$. Then, the projection of f onto the column space of $\Phi(\boldsymbol{\eta})$ can be expressed as

$$P_{\Phi(\boldsymbol{\eta})} \boldsymbol{f} = \hat{f}(\boldsymbol{\eta}) = \Phi(\boldsymbol{\eta})\Phi(\boldsymbol{\eta})^+ \boldsymbol{f}, \tag{1}$$

where $\Phi(\boldsymbol{\eta})^+$ denotes the Moore-Penrose pseudo inverse [14] of $\Phi(\boldsymbol{\eta})$. Then, the problem of identifying the optimal variable projection operator is equivalent to the minimization of the functional

$$r_2(\boldsymbol{\eta}) := \|\boldsymbol{f} - P_{\Phi(\boldsymbol{\eta})}\|_2^2 = \|\boldsymbol{f} - \Phi(\boldsymbol{\eta})\Phi(\boldsymbol{\eta})^+ \boldsymbol{f}\|_2^2. \tag{2}$$

Clearly, minimizing r_2 in (2) is an SNLLS task. Furthermore, in [14] Golub and Pereyra were the first to show that the gradient of r_2 with respect to $\boldsymbol{\eta}$ can be analytically given provided that the partial derivatives $\frac{\partial \Phi(\boldsymbol{\eta})}{\partial \boldsymbol{\eta}}$ are known. This finding allows us to minimize (2) using gradient based methods.

III. Physical background

A schematic of the CT imaging process is given in Fig. 1. Although in this work we consider 2D images, the proposed method can be applied to all possible 2D slices to obtain 3D models. Let us consider a single line segment of emitters and corresponding detectors, where each emitter-detector pair is characterised by its position along this segment: $r \in [-1, 1]$. The emitters and detectors are rotated around the object of interest, with the beams traversing between them. That is, the path of a single X-ray beam is assumed to be a line $L(r, \alpha)$, where r denotes the detector position and $\alpha \in [0, \pi)$ gives the angle of rotation. Even though in our experiments we assumed that the emitted beams are parallel, there is no theoretical constraint that prohibits the use of the proposed model with modern, fan-like beam geometry.

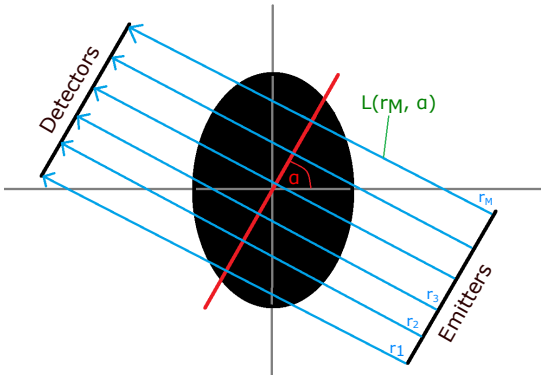

Fig. 1: CT imaging using parallel beams.

Beer's law describes a fundamental relationship between the initial and exit intensities of an X-ray beam and the attenuation properties of the examined material:

$$I_e := I_i \cdot e^{-\int_{L(r,\alpha)} \mu(t)dt}. \tag{3}$$

In (3), $I_e, I_i \in \mathbb{R}$ denote the initial and exit beam intensities, $L(r, \alpha)$ denotes the line along which the beam traverses and the function μ denotes the attenuation function that describes the examined material. In CT imaging, we are interested in finding the function μ given initial and exit intensities from many beams.

Beer's law (3) can be reformulated as

$$p(r, \alpha) = -\ln \frac{I_e}{I_i} = \int_{L(r,\alpha)} \mu(t)dt. \tag{4}$$

From (4) it is clear, that $-\ln \frac{I_e}{I_i}$ expresses the *Radon-transform* [17] of the attenuation function along the line $L(r, \alpha)$. The function $p : [-1, 1] \times [0, \pi) \to \mathbb{R}$ is referred to as the sinogram. Equation (4) also shows that the relationship between this quantity and the attenuation function is linear. This (in theory) allows for the reconstruction of the attenuation function along all possible lines using back projection [1], [2].

The linear relationship described in (3) and (4) only holds under the assumption that the emitted X-ray beams are monochromatic. In practice however, CT machines are only capable of emitting polychromatic X-ray beams [1]. Since materials attenuate lower energy photons more easily [1],

the use of polychromatic beams results in higher attenuation values around the edges of homogeneous materials in the reconstructed image. This physical phenomenon is called beam hardening and its effect is demonstrated in Fig. 2. The errors appearing on the reconstructed image due to beam hardening are usually referred to as "cupping" artifacts because of their characteristic shape. In the presence of beam hardening, equation (4) can be given by the nonlinear relationship

$$p(\alpha, r) = -\ln\left(\int_0^{E_{\max}} \rho(E) e^{-\int_{L(\alpha,r)} \mu(t,E)dt} dE\right), \quad (5)$$

where $E_{\max}$ denotes the maximum energy a photon can obtain and $\rho(E)$ denotes the probability density of a photon obtaining energy level E.

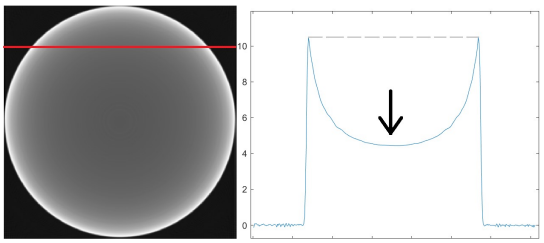

Fig. 2: Cupping artifacts. LEFT: reconstructed image in the presence of beam hardening. RIGHT: a cross section of attenuation values along the red line resembles the shape of a cup.

IV. Methods

We can obtain an approximation of the sinogram by considering a discretization of (5). Let Q, N and $M \in \mathbb{N}$ denote the number of energy levels in the emitted beams, the number of materials in the examined object and the number of detectors respectively. In addition, suppose the detectors are rotated along $O \in \mathbb{N}$ angles around the object. Although this number depends heavily on the CT machine and its settings, high quality results can be obtained with i.e. $O \approx 1000$ angles [1]. Consider a fixed rotation angle $\alpha := \alpha_j$ $(j \in \{1, \dots, O\})$ and let $l_\alpha(i,k)$ denote the length of the path of the i-th beam in the k-th material. In this work, we assume these lengths to be known a priori. If a segmentation of the examined object is available, then the values $l_\alpha(i,k)$ can be easily calculated. This always holds, when the examined object is a physical phantom. We obtain the following approximation of the sinogram (5):

$$p(\alpha, r_i) \approx \hat{p}_\alpha(r_i) = -\ln\left(\sum_{j=1}^{Q} \rho_j e^{-\sum_{k=1}^{N} \mu_{j,k} l_\alpha(i,k)}\right). \quad (6)$$

Our task is to estimate the energy level probabilities ρ_j and the attenuation coefficients $\mu_{j,k}$ $(j = 1, \dots, Q,\ k = 1, \dots, N)$. That is, we would like to get a good estimate of the attenuation properties of each material at each energy level.

As mentioned in section II, we pose the problem of finding the above mentioned parameters as an SNLLS task. To this end, consider the vector $\boldsymbol{y} \in \mathbb{R}^M$, $\boldsymbol{y}_i := e^{-\hat{p}_\alpha(r_i)}$. Then, by (6) we have

$$\boldsymbol{y}_i = \sum_{j=1}^{Q} \rho_j e^{-\sum_{k=1}^{N} \mu_{j,k} l_\alpha(i,k)}. \quad (7)$$

Using the notations from section II, we introduce the parameter vector

$$\boldsymbol{\eta} := [\mu_{1,1}, \dots, \mu_{Q,1}, \mu_{1,2}, \dots, \mu_{Q,N}]^T \in \mathbb{R}^{Q \cdot N}. \quad (8)$$

and the basis vectors

$$\varphi_{\alpha,j}(\boldsymbol{\eta}) = \left[e^{-\sum_{k=1}^{N} \mu_{j,k} \cdot l_\alpha(1,k)}, \dots, e^{-\sum_{k=1}^{N} \mu_{j,k} \cdot l_\alpha(M,k)}\right]^T \in \mathbb{R}^M, \quad (9)$$

where $j = 1, \dots, Q$. Letting $\Phi_\alpha(\boldsymbol{\eta}) \in \mathbb{R}^{M \times Q}$ be the matrix, whose columns contain the basis vectors (9) corresponding to angle α, we can formulate the parameter optimization problem in the desired SNLLS form

$$\min_{\boldsymbol{\eta} \in \mathbb{R}^{Q \cdot N}} r_{\alpha,2}(\boldsymbol{\eta}) = \min_{\boldsymbol{\eta} \in \mathbb{R}^{Q \cdot N}} \|\boldsymbol{y} - \Phi_\alpha(\boldsymbol{\eta}) \Phi_\alpha(\boldsymbol{\eta})^+ \boldsymbol{y}\|_2^2. \quad (10)$$

Note that the partial derivatives of the basis vectors $\varphi_{\alpha,j}(\boldsymbol{\eta})$ exist with respect to all components of $\boldsymbol{\eta}$ and can be easily calculated. Thus, according to the discussion in section II, the problem (10) can be solved using a gradient based numerical optimization scheme.

Finally, up until this point we assumed that the detector angle α was fixed. Considering every available detector angle $\alpha_s \in [0, \pi)$ $(s = 1, \dots, O)$, we can find the optimal model parameters by solving a single SNLLS problem defined by the overdetermined system

$$\Phi(\boldsymbol{\eta})\boldsymbol{\rho} = \begin{bmatrix} \Phi_{\alpha_1}(\boldsymbol{\eta}) \\ \Phi_{\alpha_2}(\boldsymbol{\eta}) \\ \vdots \\ \vdots \\ \Phi_{\alpha_O}(\boldsymbol{\eta}) \end{bmatrix} \cdot \begin{bmatrix} \rho_1 \\ \rho_2 \\ \vdots \\ \rho_Q \end{bmatrix} = \begin{bmatrix} \boldsymbol{y}_{\alpha_1} \\ \boldsymbol{y}_{\alpha_2} \\ \vdots \\ \boldsymbol{y}_{\alpha_O} \end{bmatrix} = \boldsymbol{y}, \quad (11)$$

where $\boldsymbol{y}_{\alpha_s}$ denotes the sinogram segment (7) corresponding to the detector angle α_s.

Once the attenuation parameters in $\boldsymbol{\eta}$ (and thus the energy level probabilities $\boldsymbol{\rho} = \Phi(\boldsymbol{\eta})^+ \boldsymbol{y}$) have been determined, there are several strategies one can use to correct cupping artifacts. These include considering the "true" attenuation for a given material to be the mean of its attenuation across all energy levels [8]: $\mu_k = \frac{1}{Q} \sum_{j=1}^{Q} \mu_{j,k}$. One could also reconstruct the image using a single attenuation coefficient $\mu_{j^*,k}$ $(k = 1, \dots, N)$, where j^* denotes the index of the highest energy-level probability. This could not be done in previous similar methods (see e.g. [6], [8], [9], [11], [12]), since they were unable to reliably estimate the attenuation parameters.

V. Experiments

We verified the effectiveness of the proposed method through numerical simulations. In particular, we considered two simulated phantoms. The first phantom represented a homogeneous material (water) and the second contained $N = 2$ materials resembling human soft tissue and bone tissue. The phantoms (with cupping) are presented in Fig. 3. All simulations were implemented using the MATLAB programming language. The forward and back projection steps of the simulations were conducted using the "radon" and "iradon" methods.

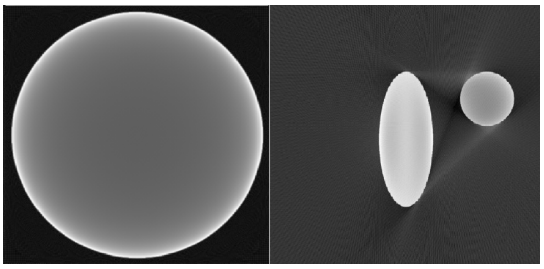

Fig. 3: Phantoms used for numerical experiments.

We conducted two types of experiments. Firstly, we were interested in measuring the proposed method's robustness against the number of energy levels considered in the X-ray beams. That is, we measured how increasing the number of energy levels Q in the beam effects the precision of the estimated attenuation coefficients in each material as well as the overall error of the reconstructed image.

We evaluated the precision of the estimated parameters using the formula

$$\mu_{MSE} := \frac{1}{Q \cdot N} \sum_{k=1}^{Q \cdot N} \left(\boldsymbol{\eta}_k^{\text{true}} - \boldsymbol{\eta}_k^{\text{est}} \right)^2, \tag{12}$$

where Q and N denote the number of energy levels and materials, while $\boldsymbol{\eta}^{\text{true}}$ and $\boldsymbol{\eta}^{\text{est}}$ denote the true and estimated attenuation coefficients as specified in (8). To measure the overall quality of the CT image, we used the mean squared error (MSE) metric [18] defined by

$$\text{MSE} := \frac{1}{R} \sum_{k=1}^{R} \left(I_k^{\text{true}} - I_k^{\text{est}} \right)^2, \tag{13}$$

where R denotes the number of pixels in the reconstructed image. In (13), I^{true} denotes the measured image and I^{est} is the image reconstructed from the modeled sinogram (6). The notation I_k denotes the row-wise indexing of the matrix I.

Fig. 4 illustrates the errors (12) and (13) for increasingly polychromatic X-ray beams. By Fig. 4, we conclude that the proposed model provides reliable estimates of the attenuation coefficients up to $4 - 5$ energy levels. In addition, the error of the reconstructed image (13) remains low (in the order of 10^{-5}) for a higher number of energy levels as well. Our experiment indicates, that it is possible to remove the cupping artifact up to $4 - 5$ energy levels in a way such that the corrected image contains Hounsfield unit (HU) values that

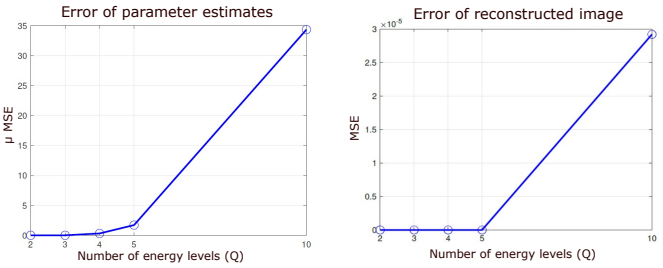

Fig. 4: Error of the estimated parameters (12) and the reconstructed image (13) for homogeneous material.

correspond to the true attenuation of the material at a given energy level (see last paragraph of section IV).

Fig. 5 shows the results of our experiments for the phantom containing multiple materials, i.e. $N = 2$.

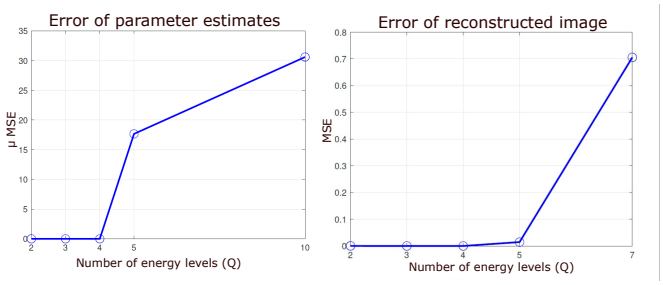

Fig. 5: Error of the estimated parameters (12) and the reconstructed image (13) for the phantom containing multiple materials.

In this case, we found that the attenuation coefficients for each material with respect to each energy level can be accurately estimated by the proposed approach if the X-ray beam contains up to 4 energy levels. Similarly to the experiments with homogeneous phantom, the error of the reconstructed image remains low, even if we assume beams with a higher number of dominant energy levels.

Our experiments show that, the proposed method is able to reliably estimate the attenuation coefficients (8) up to $Q = 4$ energy levels. This is significant for two reasons. First, previous methods [6], [8], [9], [11], [12] could not be used to estimate these parameters, they only aimed to remove the effect of beam hardening. Because of the lack of a good estimate of the attenuation parameters, the corrected image did not reflect the actual attenuation properties of the examined materials [8]. In contrast, using the estimates provided by the proposed method, it is possible to remove the cupping artifact from the measured CT image in a way that the corrected image matches the actual attenuation of the materials present in the object. Secondly, many modern CT machines use wolfram anodes to emit X-ray beams which are characterized by only $Q = 2$ dominant energy levels [1], [19]. Since our numerical experiments show the reliability of the proposed method up to $Q = 4$, our results warrant conducting experiments with real CT machines.

Finally, Fig. 6 illustrates a corrected CT image. Table I contains the true and estimated attenuation coefficients and

energy level probabilities used for the experiment in Fig. 6. Clearly, in this particular case, both the linear parameters (energy bin probabilities) and the corresponding attenuation coefficients for each material were estimated with near perfect accuracy.

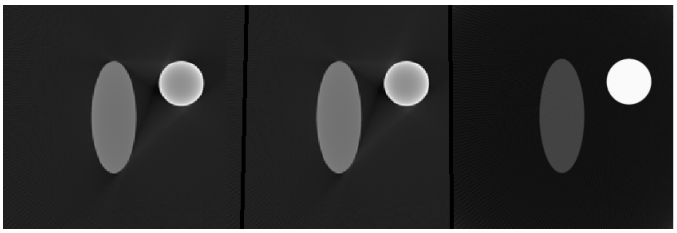

Fig. 6: Measured, approximated and corrected reconstructions for $N = 2$.

	Linear parameters		**μ material 1**		**μ material 2**	
Energy level	True	Est.	True	Est.	True	Est.
1.	0.296	0.296	3.909	3.909	8.313	8.313
2.	0.392	0.392	1.733	1.733	8.033	8.033
3.	0.311	0.311	1.331	1.331	0.605	0.605

TABLE I: True and estimated linear and nonlinear parameters used in the experiment shown in Fig. 6.

VI. Conclusion

In this work, we proposed a novel approach to model CT images in the sinogram space. We extended our previous work [13] and for the first time, we used a variable projection based adaptive method to estimate the attenuation coefficients describing a CT image in objects containing multiple materials. We found that the proposed method performs well for homogeneous phantoms and for objects containing multiple materials (provided that a segmentation is available). Our results warrant experiments with real CT machines where often $Q = 2$ dominant energy levels can be expected [1], [19]. An advantage of the proposed method over previous approaches [6], [8], [9], [11], [12] is that it is able to reliably estimate the attenuation coefficients of the investigated objects. This allows for the correction of the artifacts in a physically informative manner.

We plan to continue our research by testing the proposed method on real CT images. Since we assumed that image segmentation is known, the current method can only be used with physical phantoms. Nevertheless, the proposed method remains applicable in practice, since beam hardening properties of the CT machine are usually investigated during spectral calibration [12] with the use of physical phantoms. To apply the proposed method to CT imaging problems in more general settings, we also plan to augment the model with a priori segmentation steps. Such a modification would also allow for the continuous monitoring of beam hardening without the need for phantoms. A monitoring scheme could be used to trigger the re-calibration of the CT machine, as it is known that the X-ray spectrum can change when the CT device is in use [1].

Acknowledgment

Project no. C1748701 has been implemented with the support provided by the Ministry of Culture and Innovation of Hungary from the National Research, Development and Innovation Fund, financed under the NVKDP-2021 funding scheme. Péter Kovács was supported by the ÚNKP-23-5 New National Excellence Program of the Ministry for Culture and Innovation from the source of the National Research, Development and Innovation Fund. Project no. TKP2021-NVA-29 and K 146721 have been implemented with the support provided by the Ministry of Culture and Innovation of Hungary from the National Research, Development and Innovation Fund, financed under the TKP2021-NVA and the K_23 "OTKA" funding schemes. The authors would like to thank Richárd Gyarmati for his help with the implementation of our numerical experiments.

References

[1] H. Jiang, *Computed tomography: principles, design, artifacts, and recent advances*. Bellingham, Washington USA: SPIE and John Wiley & Sons, Inc.: SPIE, 2009.

[2] A. C. Kak and M. Slaney, *Principles of computerized tomographic imaging*. SIAM, 2001.

[3] P. Suetens, *Fundamentals of medical imaging*. Cambridge University press, 2017.

[4] L. De Chiffre, S. Carmignato, J.-P. Kruth, R. Schmitt, and A. Weckenmann, "Industrial applications of computed tomography," *CIRP annals*, vol. 63, no. 2, pp. 655–677, 2014.

[5] A. du Plessis, S. G. le Roux, and A. Guelpa, "Comparison of medical and industrial x-ray computed tomography for non-destructive testing," *Case Studies in Nondestructive Testing and Evaluation*, vol. 6, pp. 17–25, 2016.

[6] C. Martinez, J. A. Fessler, M. Desco, and M. Abella, "Simple beam hardening correction method (2dcalbh) based on 2d linearization," *Physics in Medicine & Biology*, vol. 67, no. 11, p. 115005, 2022.

[7] G. A. Rodriguez-Granillo, P. Carrascosa, S. Cipriano, M. De Zan, A. Deviggiano, C. Capunay, and R. C. Cury, "Beam hardening artifact reduction using dual energy computed tomography: implications for myocardial perfusion studies," *Cardiovascular diagnosis and therapy*, vol. 5, no. 1, p. 79, 2015.

[8] G. Van Gompel, K. Van Slambrouck, M. Defrise, K. J. Batenburg, J. De Mey, J. Sijbers, and J. Nuyts, "Iterative correction of beam hardening artifacts in CT," *Medical physics*, vol. 38, no. S1, pp. S36–S49, 2011.

[9] J. Lifton, "Multi-material linearization beam hardening correction for computed tomography," *Journal of X-ray science and technology*, vol. 25, no. 4, pp. 629–640, 2017.

[10] L. Yu, S. Leng, and C. H. McCollough, "Dual-energy CT-based monochromatic imaging," *American journal of Roentgenology*, vol. 199, no. 5_supplement, pp. S9–S15, 2012.

[11] J. Hsieh, R. C. Molthen, C. A. Dawson, and R. H. Johnson, "An iterative approach to the beam hardening correction in cone beam CT," *Medical physics*, vol. 27, no. 1, pp. 23–29, 2000.

[12] E. Y. Sidky, E. R. Paul, T. Gilat-Schmidt, and X. Pan, "Spectral calibration of photon-counting detectors at high photon flux," *Medical Physics*, vol. 49, no. 10, pp. 6368–6383, 2022.

[13] T. Dózsa, S. Fridli, and P. Kovács, "Artifact reduction in CT images," in *HU-MATHS-IN Success Stories of Mathematical Short-Term Projects for Industry in 2017-2021*, 2021, pp. 84–91.

[14] G. H. Golub and V. Pereyra, "The differentiation of pseudo-inverses and nonlinear least squares problems whose variables separate," *SIAM Journal on numerical analysis*, vol. 10, no. 2, pp. 413–432, 1973.

[15] G. Golub and V. Pereyra, "Separable nonlinear least squares: the variable projection method and its applications," *Inverse problems*, vol. 19, no. 2, p. R1, 2003.

[16] P. P. Petrushev and V. A. Popov, *Rational approximation of real functions*. Cambridge University Press, 2011, no. 28.

[17] J. Radon, "über die bestimmung von funktionen durch ihre integralwerte längs gewisser mannigfaltigkeiten," *Classic papers in modern diagnostic radiology*, vol. 5, no. 21, p. 124, 2005.

[18] C. C. Beckner Jr and C. L. Matson, "Using mean-squared error to assess visual image quality," in *Advanced Signal Processing Algorithms, Architectures, and Implementations XVI*, vol. 6313. SPIE, 2006, pp. 129–137.

[19] "Report 87," *Journal of the ICRU*, vol. 12, no. 1, pp. 55–66, 2012.